Analyst

Accepted Manuscript

This is an *Accepted Manuscript*, which has been through the Royal Society of Chemistry peer review process and has been accepted for publication.

Accepted Manuscripts are published online shortly after acceptance, before technical editing, formatting and proof reading. Using this free service, authors can make their results available to the community, in citable form, before we publish the edited article. We will replace this *Accepted Manuscript* with the edited and formatted *Advance Article* as soon as it is available.

You can find more information about *Accepted Manuscripts* in the **Information for Authors**.

Please note that technical editing may introduce minor changes to the text and/or graphics, which may alter content. The journal's standard **Terms & Conditions** and the **Ethical guidelines** still apply. In no event shall the Royal Society of Chemistry be held responsible for any errors or omissions in this *Accepted Manuscript* or any consequences arising from the use of any information it contains.

Journal Name

ARTICLE

Plasmonic sensors for the competitive detection of testosterone

H. Yockell-Lelièvre,[a] N. Bukar[a], K. S. McKeating[a], M. Arnaud[b], P. Cosin[b], Y. Guo[b], J. Dupret-Carruel[b], B. Mougin[b], and J.-F. Masson[a,c*]

The ability to detect small molecules in a rapid and sensitive manner is of great importance in the field of clinical chemistry, and the advancement of novel biosensors is key to realising point-of-care analysis for essential targets. Testosterone is an example of such a small molecule, the detection of which is important in both clinical analysis, and in the sporting industry to prevent doping. As such, a portable, rapid and sensitive test for testosterone would be of great use across a variety of analytical fields. Here we report on a novel method of testosterone analysis, based on a competitive inhibition assay utilising functionalized gold nanoparticles. Two sensing platforms are directly compared for the detection of testosterone based on both classical SPR and LSPR. We provide an in-depth discussion on the optimum surface chemistries needed to create a stable detection conjugate before successfully detecting testosterone using our newly developed portable 4-channel SPR instrument. We provide the first detailed study into the comparison of SPR and LSPR for the analysis of a small molecule, and provide a simple and effective method of testosterone detection that could potentially be extended to a variety of different analytes.

Introduction

Biosensors have gained broad acceptance in analytical sciences for applications ranging from clinical chemistry to environmental monitoring. Specifically, they have been developed for several ions [1, 2], small molecules [3, 4], larger biomolecules and cells. Despite this broad applicability, biosensing of small molecules remains challenging, as the sensitivity of many biosensing techniques is proportional to the mass of the analyte, rendering the detection of small molecules difficult by comparison. Therefore, the majority of biosensors are applied to larger biomolecules such as DNA, proteins and antibodies, due to their larger mass and the availability of biomolecular receptors for these molecules.

Small molecules include drugs, metabolites, hormones, lipids, sugars, and nucleosides, among others, and are all analytes of great importance in clinical chemistry. However, biochemical tests for such analytes are still performed in centralized laboratories often using time-consuming tests on large instrumentation. The development of small and portable biosensors for common biochemical tests would provide a faster, inexpensive solution to personalized medicine.

Plasmonic sensors, comprised of classical surface plasmon resonance (SPR) and localized surface plasmon resonance (LSPR) biosensors, have recently attracted significant attention due to their broad applicability, simplicity of measurement,

high sensitivity, and suitability for point-of-care applications. Plasmonic biosensors rely on small, albeit measureable, refractive index changes in the vicinity of gold or silver in the form of thin films (SPR), nanoparticles or nanostructures (LSPR). Molecular receptors immobilized to the plasmonic substrate imparts the selectivity of these biosensors for direct detection, secondary detection, competition and inhibition competition assays [5]. Additionally, plasmonic sensors can be easily scaled down to small devices, and using these principles, a small and portable 4-channel SPR biosensor was recently developed for the competitive monitoring of methotrexate, a common anti-cancer agent used in many chemotherapy treatments [6]. Clinical chemistry applications could benefit from this small and portable SPR biosensor for other analytes of interest.

Testosterone is an important analyte in both clinical chemistry and for anti-doping programmes in sport. The importance of testosterone sensing, along with its low concentration in biofluids, makes this analyte an excellent model to develop sensing technologies for small molecules. In recent years, different sensing strategies and a series of biosensing techniques have been proposed to quantify testosterone using bimolecular or synthetic receptors (Table S1). Testosterone sensors based on electrochemistry [7-12], spectroscopy [13-20] or radiolabelling [21] assays typically have detection limits in the high picomolar region (Table S1),

whereas lower detection limits have been achieved using molecularly imprinted polymers (MIP), [11, 12] and stochastic electrochemical sensors [14, 15] allowing for detection limits in the femtomolar region.[19-21] These concentrations, although extremely sensitive, are unsuitable for clinical chemistry applications where the concentration of testosterone is typically in the high picomolar to low nanomolar range.

Clinical chemistry applications require both low detection limits and high sensitivity for providing accurate measurements. While the sensitivity of plasmonic sensors is generally high, it can be further increased with the use of gold nanoparticles in certain biosensing applications [22]. Based on these principles, Mitchell *et al.* developed an inhibition competition assay between free testosterone and anti-testosterone coupled to a gold nanoparticle in solution for a testosterone-modified SPR sensor [18]. Herein, we report on a direct competition assay between testosterone and a testosterone-modified Au nanoparticle (Au NP) for anti-testosterone immobilized directly on an SPR or LSPR plasmonic sensor. Different surface chemistries were tested to optimize the colloidal stability and sensitivity of the detection Au NP for testosterone. This testosterone assay was then tested with a 4-channel instrument suited for both classical SPR and LSPR measurements and the performance was compared for the two detection schemes. This provides the first direct comparative study of SPR and LSPR for small molecule detection.

Experimental

Synthesis of testosterone biotin derivative

The NMR spectra were recorded in $CDCl_3$ with a Bruker AV 250 spectrometer at 62.8 MHz (^{13}C). Chemical shifts are reported in parts per million (ppm) downfield from Me_4Si. Analytical TLC was performed on 0.2 mm silica gel 60F254 (Merck) aluminum supported plates. Detection was achieved by spraying with 10% (v/v) sulfuric acid in MeOH and heat charring. Column chromatography on silica gel 60 was used to purify the product. N-(+)-Biotinyl-3-aminopropylammonium trifluoroacetate (100 mg, 0.241 mmole) was added to 4.5 mL of a 1 M solution of sodium bicarbonate and stirred at room temperature for 1 h. The resulting mixture was used without further processing in the next step. To a solution of the acid **1** [23] (100 mg, 0.287 mmole) in 7 mL of anhydrous 1,2-dimethoxyethane, N-hydroxysuccinimide (NHS, 50 mg, 0.434 mmole) was added. After stirring at room temperature for 3 min, N,N'-Dicyclohexylcarbodiimide (DCC, 69 mg, 0.334 mmole) was added and stirred at room temperature for 18 h. The mixture was filtered and the crude product **3** was added to this solution. The reaction was left to continue for 14 h at room temperature. The reaction mixture was concentrated at room temperature and the residue was purified by column chromatography on silica gel (dichloromethane/methanol, 8/1, v/v) to give 125 mg (82%) of **4** as white powder. ^{13}C NMR ($CDCl_3$): 173.3, 171.1, 163.8, 149.0, 119.8, 81.7, 76.3, 66.9,
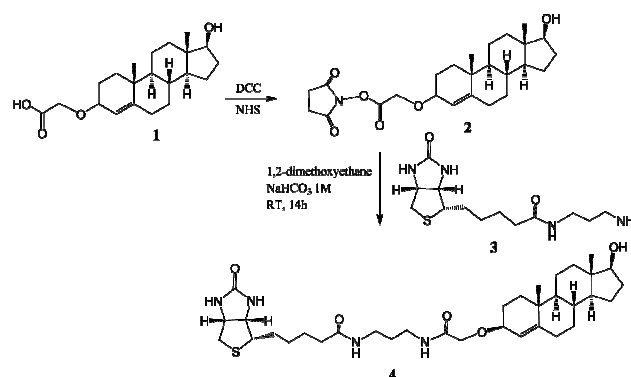
Figure 1. Synthetic route of testosterone biotin derivative

61.6, 60.1, 55.5, 54.4, 50.6, 42.8, 40.5, 37.6, 36.5, 36.1, 35.9, 35.7, 35.5, 35.0, 32.5, 32.1, 30.4, 29.5, 28.2, 28.0, 25.6, 25.4, 23.3, 20.5, 18.8, 11.1.

Synthesis of the Au nanoparticles used for the fabrication of the LSPR sensors

Ultrapure Millipore water (18.2 MΩ cm^{-1}) was used for all nanoparticle synthesis. All glassware was washed with aqua regia (Caution, aqua regia is highly corrosive!) and rinsed with ultrapure water. 60 nm Au NP's were synthesized using a seeded growth method. 15 nm seeds were obtained by mixing 0.3 g of trisodium citrate dihydrate and 40 mg of hydrogen tetrachloroaurate trihydrate ($HAuCl_4.3H_2O$) in 1L of water at room temperature, and bringing to the boil in a 1000 W commercial microwave oven for 5 minutes. 15 mL of the room-cooled seeds sol and 3 mL of a 200 mM solution of hydroxylamine were added to 400 mL of water. 5 mL of a 50 mM solution of $HAuCl_4.3H_2O$ was added dropwise to this solution under constant stirring and let to stir for 5 minutes. The suspension was then concentrated by centrifugation at 15 000 RPM for 2 min. The Au NP's were then coated with thiol-terminated polystyrene (PS, Mn=8000 g/mol) via ligand exchange in acetone.

Synthesis of the detection Au nanoparticle

25 nm Au NP's were synthesized using a slightly modified version of the protocol developed by Xie and al.[22]. 70 nm branched nanoparticles were first synthesized by mixing 2.5 mL of a 50 mM solution of $HAuCl_4.3H_2O$ and 25 mL of a 0,1 M solution of HEPES (previously adjusted to pH 7.4) into 500 mL of water and stirring for 1 hour at room temperature. The suspension was then heated for 5 minutes in a 1000 W commercial microwave oven in order to induce Ostwald ripening of the particles, resulting in spherical, 25 nm Au NP's. The suspension was then concentrated by centrifugation at 15 000 RPM for 2 min. These particles showed better stability upon further functionalization than the ones produced via seeded growth.

Analyst Accepted Manuscript

1
2
3
4
5
6
7
8
9
10
...
60

Detection Au NP's were directly functionalized with either testosterone-biotin or a thiolated linker (11-mercaptoundecanoic acid (MUA), 11-mercaptoundecane-triethylglycol acid (MUPEGA) or 3-MPA-LHDLHD-OH). Functionalization with testosterone-biotin was carried out as follows: 3 mL of the concentrated 25 nm Au NP's were added dropwise to 50 mL of a 20 Ҡg / mL solution of testosterone-biotin in ethanol under constant stirring in an ice bath. After 15 minutes, 5 mL of a 10 mM solution of folic acid in ethanol was added in order to stabilize the unreacted surface. Functionalization with a linker was carried out as follows: 3 mL of the concentrated 25 nm Au NP's were added dropwise to 50 mL of a 10 mM solution of thiolated linker in ethanol under constant stirring. In both cases, after 1 hour of stirring, the suspension was centrifuged at 15 000 RPM for 1 minute and re-suspended in clean ethanol under sonication. This cycle was repeated three times, and the sample dried with a flow of nitrogen.

Further functionalization of the linker-capped Au NP's with anti-biotin was carried out by re-suspending the dried Au NP's in 2 mL of water and quickly adding to 10 mL of a fresh mixture of EDC (39 mg / mL) and NHS (14 mg / mL) under constant stirring in a closed glass vial, and let to react for 20 minutes with occasional sonication. The mixture was then centrifuged and rinsed once with water and once with PBS pH 4.5. The Au NP's were then re-suspended in 5mL of a 20 Ҡg / mL solution of anti-biotin in PBS pH 7.4 and left to react overnight at 4°C. After centrifugation, the Au NP's were re-suspended in 1 M ethanolamine pH 8.5 and left to react for 5 minutes in order to block unreacted carboxyl groups on the linkers. The samples were then rinsed twice with water and re-suspended in PBS pH 7.4. Testosterone-biotin-functionalized Au NP's were re-suspended in PBS pH 7.4 prior to use.

SPR and LSPR Measurements

SPR and LSPR experiments were performed on a portable 4-channel SPR instrument based on a dove prism design previously reported [6, 24]. Experiments were carried out using the wavelength interrogation configuration of SPR, with a working range of 550 to 850 nm (Ocean Optics USB4000 with a grating centred at 700 nm). LSPR measurements were carried out from 450 to 750 nm. In this case, the instrument was modified with a different spectrophotometer (Ocean Optics USB4000 with a grating centred at 600 nm). Data was acquired and processed in real-time with Labview software.

SPR and LSPR sensors preparation

Dove prisms (20 x 12 x 3 mm) were cleaned in piranha solution (90 min at 80°C). The dove prisms were then coated with 1 nm Cr and 50 nm Au to create the SPR sensors. The LSPR sensors were fabricated by spreading and drying a small droplet of a concentrated (~10^{14} NP/mL) suspension of PS-capped 60 nm Au NP's in chloroform onto the surface of the dove prism. The chloroform solution also contained excess unbound PS to ensure that no plasmon coupling occurs between neighbouring Au NP's in the sensing layer. The PS was removed by etching with an oxygen plasma for 2 hours. The surface of both the SPR and LSPR sensors were functionalized with 3-MPA-LHDLHD-OH by submerging the prisms in a 2 mg / mL solution of the peptide in ethanol overnight. The prisms were then cleaned with ethanol and de-ionized water. The carboxyl groups on the surface were activated by manually injecting a 300 µL solution of EDC (39 mg / mL) and NHS (14 mg / mL) onto the surface of the prisms for 20 minutes, before washing with de-ionized water and PBS pH 4.5. For the SPR sensor 300 µL of 10 µg / mL anti-testosterone in PBS pH 7.4 was injected onto the sensor surface and binding monitored in real time via SPR for 15 minutes. For the LSPR sensor the prisms were submerged in a solution of 10 µg / mL anti-testosterone in PBS pH 7.4 and was reacted at room temperature for 10 minutes before storing overnight at 4°C. Unreacted linkers were blocked using 1 M ethanolamine pH 8.5.

Testosterone sensing

Testosterone was detected using both the SPR and LSPR surfaces modified with 3-MPA-LHDLHD-OH and anti-testosterone as previously described. A solution of 10 ng/mL testosterone-biotin was pre-mixed with varying concentrations of free testosterone in PBS (0.05 to13 ng/mL). 300 µL of this mixture was injected into the 4-channel SPR and reacted with the surface for 15 minutes. 300 µL of the Au NP-MUPEGA-anti-biotin conjugate was injected at a concentration of 5×10^{12} NP/mL for 20 minutes, and the shift in SPR wavelength over time recorded.

Results and discussion

The testosterone plasmonic sensors developed were based on the competition of free testosterone (the analyte) with a testosterone-biotin competitor (Figure 2). A Au NP modified
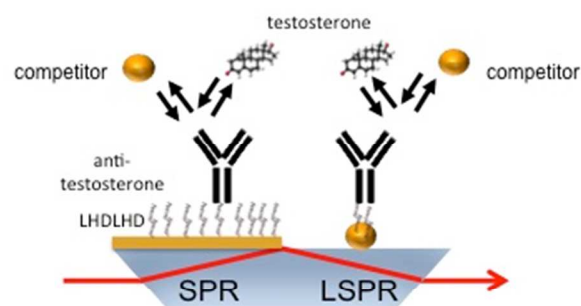
Figure 2. SPR and LSPR sensing scheme of testosterone. The SPR sensor was based on a thin gold film on the dove prism, while the LSPR sensor was created by immobilizing a monolayer of Au nanospheres on the dove prism. Anti-testosterone was immobilized on the SPR and LSPR sensors, and the free testosterone and conjugated testosterone-biotin compete for the surface.
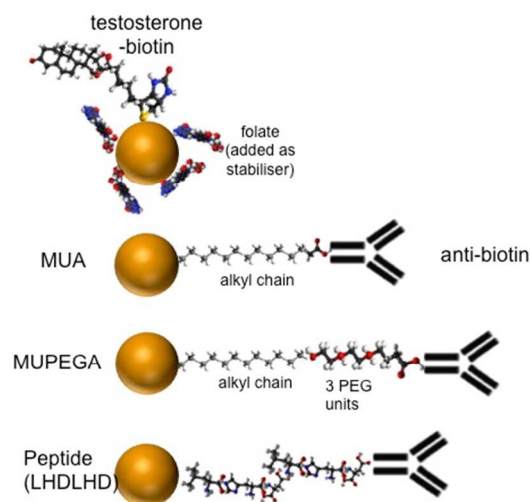
Figure 3. Detection Au NP with varying surface chemistries.

with testosterone-biotin (either directly or with anti-biotin) formed the basis of the competition assay on both the SPR and LSPR sensors. Gold nanoparticles are used to enhance the signal in classical SPR analysis via a combination of an increased mass on the surface, and as a result of plasmonic coupling between the nanoparticle and the gold surface. As such, in the absence of a testosterone molecule to compete with, all functionalized nanoparticles should bind to the biosensor surface, providing a high signal enhancement. When high concentrations of testosterone are introduced, the competitor concentration binding to the plasmonic sensor is decreased, and thus a lower response is observed.

The testosterone-biotin competitor (Figure 1, compound **4)** was synthesized via a biotinylation reaction between commercially available N-(+)-Biotinyl-3-aminopropyl-ammonium trifluoroacetate and the active ester **2** which was prepared according to a previously reported procedure [23] using testosterone as the starting material (Figure 1). This biotinylated testosterone derivative **4** is a K-isomer in the C_3 position of testosterone with a spacer of 7 atoms between testosterone and biotin.

The plasmon resonance was measured in total internal reflection using the 4-channel SPR instrument previously described. This instrument was competent for monitoring both the plasmon resonance of the classical SPR sensors on a thin Au film, and of the novel LSPR sensors.

Detection gold nanoparticle for testosterone sensing

The surface chemistry on the gold nanoparticles will dictate the colloidal stability of the detection conjugate and therefore Au NP's of 25 nm in size were functionalized with varying linkers to optimize this stability. The detection nanoparticles were reacted either directly with testosterone-biotin, or with a carboxylated thiol linker and anti-biotin (Figure 3) to fully
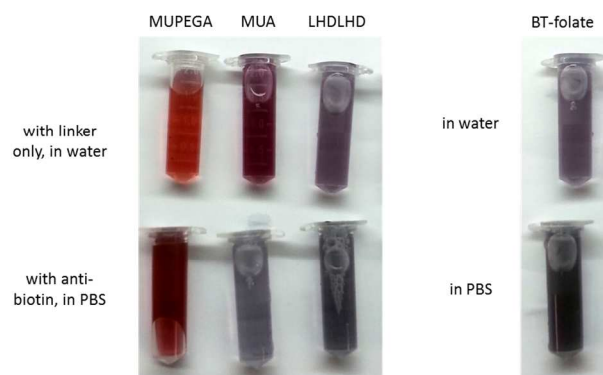
Figure 4. Photographs of the Au NP solutions with the monolayer only in water and modified with anti-biotin in PBS (left) and Au NP's modified directly with testosterone-biotin and folate in water and PBS (right).

assess optimum conditions. The linkers chosen included 11-mercaptoundecanoic acid (MUA) as a common alkane thiol used to form an SAM on gold, 11-mercaptoundecane-triethylglycol acid (MUPEGA) as a method of investigating a larger linker on the stability and finally a peptide monolayer consisting of the amino acids leucine (L) histidine (H) and aspartic acid (D) with a mercaptopropanoic acid moiety (3-MPA-LHDLHD-OH) which has been previously shown to reduce non-specific binding on SPR sensors [25]. The colloidal stability of the Au NP's functionalized with these monolayers was evaluated using UV-Vis spectroscopy (Figure S1). The addition of both MUA and 3-MPA-LHDLHD-OH to the nanoparticle surface caused a bathochromic shift from 525 nm to 538 nm and 556 nm, respectively. (Figure S1A) This was accompanied by a broadening of the plasmon band and a visual colour change from red to purple (Figure 4) for both monolayers indicating instability of the nanoparticles. The addition of MUPEGA, however, resulted in relatively stable nanoparticles demonstrated by the comparatively sharp band in the UV-Vis spectrum and lack of colour change after monolayer functionalization (Figure S1B and Figure 4).

The Au NP's with varying monolayers were then functionalized with anti-biotin via standard EDC/NHS coupling chemistry to activate the COOH groups of the monolayers, and reaction with ethanolamine to deactivate any unreacted functional groups after anti-biotin attachment. Anti-biotin was selected in the detection scheme due to its high specificity of reaction and the prevalence of protocols for the immobilization of antibodies to Au NP. The Au NP's were then capped with BSA to stabilise them in solution and reduce any non-specific binding that may occur. The UV-Vis spectra acquired after anti-biotin attachment demonstrated significant aggregation of the nanoparticles with MUA and 3-MPA-LHDLHD-OH monolayers, indicated by the high absorbance at 700 nm and also by the blue colour of the colloidal suspension (Figures 4 and S1A). The MUPEGA monolayer modified with anti-biotin was the only functionalization protocol that resulted in stable Au NP's, as demonstrated by a plasmon band at 537 nm and
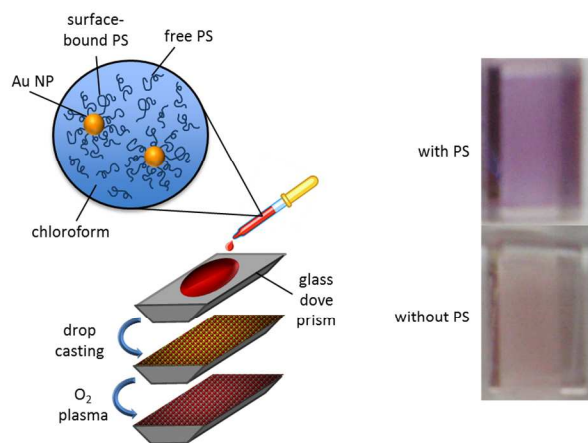
Figure 5. Left) Schematic of the synthesis of the LSPR sensor surface. Right) Pictures of the LSPR sensor with polystyrene-capped Au nanospheres of 60 nm diameter (top) and bare 60 nm Au nanospheres (bottom). The colour of the prism changed from purple for the Au NP's capped with polystyrene to blush pink for bare Au NP's.

red colour in PBS, and thus this linker was taken forward into further experimentation and the detection of testosterone.

Additionally, in an attempt to create nanoparticles modified directly with a testosterone-biotin complex, the biotin moiety was directly physisorbed onto the Au NP surface to create the testosterone competitor. However, the charge of the Au NP dropped significantly as testosterone-biotin is neutral, and thus the Au NP's aggregated rapidly out of solution. Adding 10 mM folate after the testosterone-biotin complex improved the colloidal stability of the Au NP's, however, significant aggregation was still visible as indicated by the dark purple colour of the Au NP's in both water and PBS (Figure 4). As a result when Au nanoparticles with testosterone-biotin/folate were used in the assay for testosterone detection they had minimal interaction with the surface, resulting in comparably low shifts, which could be the result of the Debye length effect as observed with our MTX assay [26].

Plasmonic sensors for testosterone

The SPR sensor was created according to a standard protocol by sputter coating a layer of chromium and a layer of gold onto custom-built glass dove prisms, previously cleaned with piranha solution. The LSPR sensor was fabricated by drop-casting polystyrene-capped 60 nm Au nanospheres onto the dove prism (Figure 5). The Au nanospheres were spread on the surface of the prism to form a monolayer, before oxygen plasma was used to remove the polystyrene capping leaving the bare surface of the Au NP exposed. This process visually changed the colour of the surface from purple to blush pink (Figure 5) and the plasmon resonance wavelength from 577 to 524 nm (in air). It was established by TEM and SEM observations that plasma treatment had no effect on the size or structure of the Au NPs.

The surface of both the SPR and LSPR biosensor was modified with 3-MPA-LHDLHD-OH, and the carboxyl groups

activated via EDC/NHS coupling chemistry. The anti-testosterone was then reacted with the monolayer, at a concentration known to result in sufficient surface coverage, completing the biosensor surface. The experimental details for the competition assay were then investigated on the LSPR sensor to optimize the response obtained. Two different detection schemes were investigated for testosterone detection, the first of which involved pre-reacting testosterone-biotin with the Au NP's functionalized with MUPEGA and anti-biotin before injection onto the sensor surface. In this assay development step it was important to assess the maximum response that could be obtained and so free testosterone was omitted in order to enable unhindered binding of the competitor conjugate to the surface. Unfortunately, the response obtained after injection of the gold nanoparticles bound to the testosterone-biotin complex was very weak and exhibited a shift of only 0.8 nm. It seems that in this detection scheme the testosterone unit of the testosterone-biotin complex is no longer available for binding to the anti-testosterone surface. In the second detection scheme the testosterone and testosterone-biotin complex would first compete for the sensor surface, and then anti-biotin functionalized nanoparticles would be introduced in a second step, enhancing the signal only when there are sufficient binding sites to the testosterone-biotin complex. Again, for the purpose of optimization this was carried out in the absence of free testosterone and a solution of testosterone-biotin was injected onto the sensor surface before the introduction of the detection gold nanoparticle conjugate. This provided much more promising results with a shift in SPR wavelength of approximately 5.4 nm, and therefore this detection format was taken forward into testosterone sensing on both the SPR and LSPR sensors.

An additional experimental parameter that required optimization was the concentration of testosterone-biotin needed to act as a successful competitor in solution. Several testosterone-biotin concentrations between 5 ng/mL and 10 µg/mL were tested (Figure S2). While high concentrations of testosterone-biotin lead to larger signals, the concentration would far exceed the concentration of free testosterone in potential clinical samples. The competitive assay would heavily favor testosterone-biotin and lead to poor detection limits, and therefore an intermediate concentration of 10 ng / mL was determined to be the optimum concentration for this purpose, being in the range of the maximum target concentration of testosterone that we wished to detect. The concentration of the detection Au NP was varied to generate the largest response for the assay (Figure S3). The LSPR response saturated with a concentration of Au NP of 5×10^{12} NP/mL. These conditions were used for the LSPR and SPR assays for testosterone.

Performance of the plasmonic sensors for testosterone sensing

The SPR and LSPR sensors were tested with a series of testosterone solutions in PBS at concentrations between 0.05 and 13 ng/mL. The absolute response was greater for the SPR than for the LSPR sensor throughout the calibration range
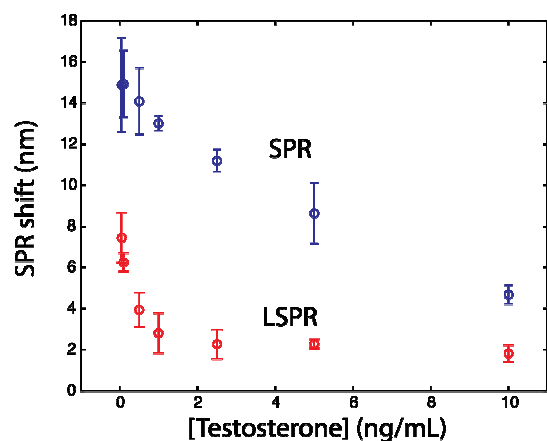
Figure 6. Comparison of the SPR and LSPR sensor for the detection of testosterone. Error bars represent one standard deviation based on 3 replicates from one SPR or LSPR surface.

(Figure 6). The calibration curve was constructed with the LSPR shift after 15 minutes of detection time (t = 1600 s in Figure 6 due to 400 s stabilisation in PBS). The dynamic range of the SPR sensor was from 0.1 to 10 ng/mL while the LSPR sensor showed enhanced signals between 0.05 and 1 ng/mL, with lower signals from 1 to 13 ng/mL. The higher concentrations of testosterone were still successfully detected with LSPR sensing, albeit with lower sensitivity, and the sensorgrams and the log-base calibration curve for LSPR show that this sensor can still discriminate between higher concentrations of testosterone (Figure 7). The relatively short dynamic range for the SPR and LSPR sensor for testosterone is a consequence of the competition assay. For the higher concentration range (greater than 1 ng/mL), the sensitivity of the SPR sensor was -1.03 nm/(ng/mL), while the LSPR sensor displayed a lower sensitivity at -0.089 nm/(ng/mL). In the concentration region lower than 1 ng/mL, LSPR showed a higher sensitivity at -4.6 nm/(ng/mL) compared to -1.03

nm/(ng/mL) for SPR. Thus, the SPR sensor is more suited to the detection of a wide concentration range, while the LSPR sensor is more sensitive towards lower concentrations. The difference observed between signal enhancement for SPR and LSPR is most likely the result of varying plasmonic field depths between the two surfaces, however, this will require further experimentation to confirm this theory.

The reproducibility of the data was slightly better for the SPR sensor. The coefficients of variation (CV) were obtained from triplicate measurements. The CV for SPR sensing ranged from 3% to 17%, with the highest CV values generally occurring at the lower and higher end of the concentration range. The LSPR sensor showed CV's from 7% to 34%. The replicability (three runs of three measurements) was measured with the SPR sensor at 23%. The LOD was calculated as the response exceeding three standard deviations from a blank measurement. The LOD was 0.05 ng/mL or 0.17 nM, which is within the concentration range of testosterone commonly used in clinical analysis. Lastly, the specificity of anti-testosterone was tested with the VIDAS® platform for 5α-androstan-17β-ol-3-one, 5α-dihydrotestosterone, 4-androstene-3,17-dione, dehydroepiandrosterone, dehydroepiandrosterone sodium sulfate, danazol, and ethisterone. Anti-testosterone responded at a relative ratio below 2 % for these interferents. These results indicated excellent specificity for the testosterone assay.

Conclusions

In conclusion, we have directly compared, for the first time, an SPR and LSPR sensor for the detection of testosterone. Using a competitive assay format and functionalized gold nanoparticles, we were able to successfully detect testosterone using a portable SPR instrument, providing a rapid and simple method of analysis. Direct comparison of the two different biosensor surfaces revealed that SPR is more amenable to testosterone detection over a wide concentration range, while LSPR is successful in the detection of low concentrations.
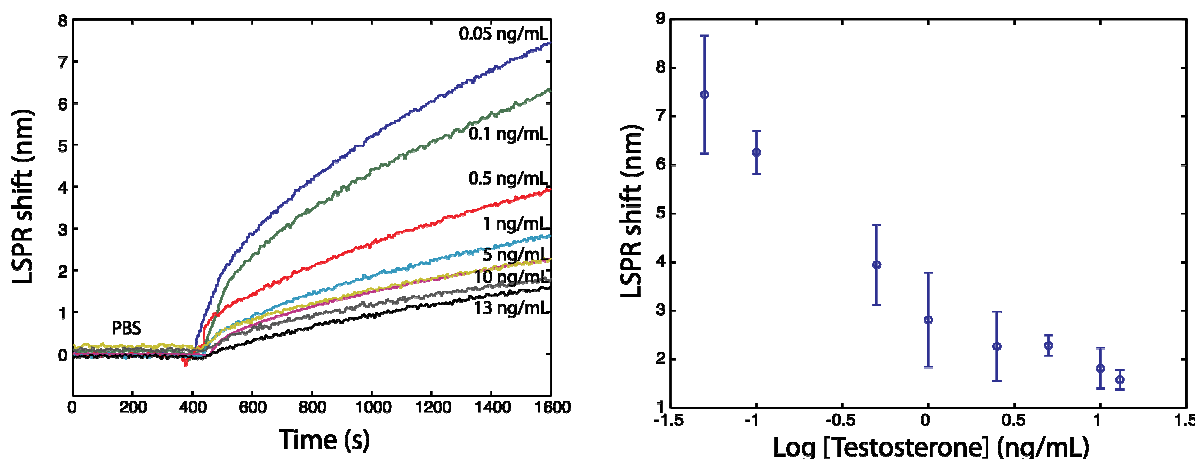
Figure 7. Left) Real time LSPR sensorgrams for testosterone. Right) log-scale calibration curve for testosterone showing increased sensitivity at higher concentrations. The shift for each individual concentration was taken at 1600 seconds. Error bars represent one standard deviation based on 3 replicates from one LSPR prism.

These simple sensors for use alongside this 4-channel SPR instrument could be applied to a wide variety of targets to provide novel, label-free methods of analysis in real time.

Acknowledgements

Notes

[a] Departement de chimie, Université de Montréal, CP 6128 Succ. Centre-Ville, Montreal, QC, Canada, H3C 3J7.

[b] BioMérieux, 376 Chemin de l'Orme, 69280 Marcy-l'Étoile, France.

[c] Centre for self-assembled chemical structures (CSACS).

[*] Corresponding author contact information: tel: +1-514-343-7342; email: jf.masson@umontreal.ca

References

1. J. Liu, *Trac-Trends in Analytical Chemistry*, 2014, **58**, 99-111.

2. W. T. D. Lin, P.-J. J. Huang, R. Pautler and J. Liu, *Chemical Communications*, 2014, **50**, 11859-11862.

3. J. Mitchell, *Sensors*, 2010, **10**, 7323-7346.

4. N. Sanvicens, I. Mannelli, J. P. Salvador, E. Valera and M. P. Marco, *Trac-Trends in Analytical Chemistry*, 2011, **30**, 541-553.

5. J. Homola, *Chemical Reviews*, 2008, **108**, 462-493.

6. S. S. Zhao, N. Bukar, J. L. Toulouse, D. Pelechacz, R. Robitaille, J. N. Pelletier and J.-F. Masson, *Biosensors & Bioelectronics*, 2015, **64**, 664-670.

7. S. L. Moura, R. R. de Moraes, M. A. Pereira dos Santos, M. Isabel Pividori, J. A. Dantas Lopes, D. d. L. Moreira, V. Zucolotto and J. R. dos Santos Junior, *Sensors and Actuators B-Chemical*, 2014, **202**, 469-474.

8. H. Lu, M. P. Kreuzer, K. Takkinen and G. G. Guilbault, *Biosensors & Bioelectronics*, 2007, **22**, 1756-1763.

9. K.-Z. Liang, J.-S. Qi, W.-J. Mu and Z.-G. Chen, *Journal of Biochemical and Biophysical Methods*, 2008, **70**, 1156-1162.

10. G. Conneely, M. Aherne, H. Lu and G. G. Guilbault, *Analytica Chimica Acta*, 2007, **583**, 153-160.

11. R.-I. Stefan-van Staden, L. A. Gugoasa, B. Calenic and J. Legler, *Scientific Reports*, 2014, **4**.

12. L. A. Gugoasa, R.-I. Stefan-van Staden, B. Calenic and J. Legler, *Journal of Molecular Recognition*, 2015, **28**, 10-19.

13. A. V. Zherdev, N. A. Byzova, V. A. Izumrudov and B. B. Dzantiev, *Analyst*, 2003, **128**, 1275-1280.

14. Q. Zhang, L. Jing, J. Zhang, Y. Ren, Y. Wang, Y. Wang, T. Wei and B. Liedberg, *Analytical Biochemistry*, 2014, **463**, 7-14.

15. Q. Wei, T. Wei and X. Wu, *Chemistry Letters*, 2011, **40**, 132-133.

16. J. Tschmelak, M. Kumpf, N. Kappel, G. Proll and G. Gauglitz, *Talanta*, 2006, **69**, 343-350.

17. S. Rau and G. Gauglitz, *Analytical and Bioanalytical Chemistry*, 2012, **402**, 529-536.

18. J. S. Mitchell and T. E. Lowe, *Biosensors & Bioelectronics*, 2009, **24**, 2177-2183.

19. S. C. Huang, G. B. Lee, F. C. Chien, S. J. Chen, W. J. Chen and M. C. Yang, *Journal of Micromechanics and Microengineering*, 2006, **16**, 1251-1257.

20. Y. Fuchs, S. Kunath, O. Soppera, K. Haupt and A. G. Mayes, *Advanced Functional Materials*, 2014, **24**, 688-694.

21. B. T. S. Bui and K. Haupt, *Journal of Molecular Recognition*, 2011, **24**, 1123-1129.

22. K. Saha, S. S. Agasti, C. Kim, X. N. Li and V. M. Rotello, *Chemical Reviews*, 2012, **112**, 2739-2779.

23. *P. Cosin and Y. Guo, "Testosterone derivatives with a carboxyalkyl substitution in position 3 and use thereof for the production of labelled steroids for determining the concentration of testosterone in a biological sample " France Patent, 2014.*

24. O. R. Bolduc, L. S. Live and J.-F. Masson, *Talanta*, 2009, **77**, 1680-1687.

25. O. R. Bolduc, P. Lambert-Lanteigne, D. Y. Colin, S. S. Zhao, C. Proulx, D. Boeglin, W. D. Lubell, J. N. Pelletier, J. Fethiere, H. Ong and J.-F. Masson, *Analyst*, 2011, **136**, 3142-3148.

26. N. Bukar, S. S. Zhao, D. M. Charbonneau, J. N. Pelletier and J.-F. Masson, *Chemical Communications*, 2014, **50**, 4947-4950.

Analyst Accepted Manuscript